Published in final edited form as:
*Stroke*. 2010 June ; 41(6): 1271–1277. doi:10.1161/STROKEAHA.109.575662.

# Molecular MRI of intracranial thrombus in a rat ischemic stroke model

**Ritika Uppal, Ph. D.**[1], **Ilknur Ay, M. D., Ph. D.**[1,*], **Guangping Dai, Ph. D.**, **Young Ro Kim, Ph.D.**, **A. Gregory Sorensen, M. D.**, and **Peter Caravan, Ph. D.**[*]
Athinoula A. Martinos Center for Biomedical Imaging, Department of Radiology, Massachusetts, General Hospital and Harvard Medical School, Charlestown, MA 02129

## Abstract

**Background and Purpose—**Intracranial thrombus is a principal feature in most ischemic stroke, and thrombus location and size may correlate with outcome and response to thrombolytic therapy. EP-2104R, a fibrin-specific molecular MR agent, was previously shown to enhance extracranial thrombi in animal models and recently, in clinical trials. The purpose of this work was to determine if a fibrin-specific molecular MR probe could noninvasively characterize intracranial thrombi.

**Methods—**Embolic stroke was induced in adult rats by occlusion of the right internal carotid artery with an aged thrombus. Diffusion weighted imaging, time of flight angiography, and high resolution three dimensional T1-weighted MRI were performed at 4.7T prior to and following contrast agents EP-2104R (10 μmol/kg, n=6) or Gd-DTPA (200 μmol/kg, control, n=5). Gd levels in thrombus, brain, and blood were determined by ex vivo elemental analysis.

**Results—**In all animals, MR angiography revealed a flow deficit and diffusion-weighted imaging showed a hyperintensity consistent with ischemia. EP-2104R-enhanced MRI resulted in visualization of all occlusive thrombi (6/6) as well as vessel wall enhancement in all 6 animals with high contrast to noise relative to blood (10.7 post EP-2104R vs. 0.54 pre, $p<0.0001$). Gd-DTPA injected animals showed no occlusive thrombus or vessel wall enhancement (0/5). The concentration of Gd in the thrombus post-EP2104 was 18 times that in the blood pool.

**Conclusions—**EP-2104R enhanced MRI successfully identifies intracranial thrombus in a rat embolic stroke model.

### Keywords

thrombus; ischemic stroke; molecular imaging; fibrin; gadolinium

## Introduction

Stroke is the second leading cause of mortality worldwide,[1] and ischemic stroke represents 85% of strokes in the western world. Imaging with CT or MRI is well established in stroke workup to distinguish ischemic from hemorrhagic stroke, to select patients for thrombolysis, and for assessment of prognosis. The culprit thrombus is sometimes observed as a hyperdense

[*]Correspondence: Ilknur Ay, Athinoula A. Martinos Center for Biomedical Imaging, Department of Radiology, Massachusetts General Hospital -East, 149 13th Street, Suite, 2301, Charlestown, MA, O2129, USA. Fax: 617-726-7422, Phone: 617-724-1145, iay@partners.org, Peter Caravan, Athinoula A. Martinos Center for Biomedical Imaging, Department of Radiology, Massachusetts General Hospital -East, 149 13th Street, Suite, 2301, Charlestown, MA, O2129, USA. Fax: 617-726-7422, Phone: 617-643-0193, caravan@nmr.mgh.harvard.edu.
[1]Ritika Uppal and Ilknur Ay contributed equally into this work.

**Conflicts of Interest:** A full listing of A.G.S.'s competing interests is available at www.biomarkers.org.

sign on non-contrast CT. The presence of either a hyperdense sign in the middle cerebral artery (MCA),[2, 3] basilar artery[4], or posterior cerebral artery[4, 5], or the hyperdense "dot" sign in the MCA[6] all demonstrate high specificity (95 – 100%) for thrombus. However the sensitivity of this sign ranges from 30 – 70%.[2–6] Hyperdense MCA is associated with poor outcome,[7] but patients may benefit from intravenous or intraarterial tissue plasminogen activator (tPA).[7–9] The hyperdense sign is believed to result from increased red cell content in the thrombus. Given that the action of tPA ultimately results in fibrinolysis, a direct molecular imaging technique to assess thrombus size and fibrin content may be useful in predicting response to thrombolysis and/or in estimating the dose of tPA required for lysis. Visualization of thrombus could also contribute to understanding the pathophysiology of stroke in a given patient, particularly post-therapy; patterns of intracranial thrombus distribution could aid determination of the stroke etiology; and visualization of any residual source thrombus outside the brain may aid in secondary stroke prevention. Because visualization of clot could have such potential, many groups have worked to create targeted agents. Nuclear medicine-based approaches have not been widely accepted to date, largely due to limited spatial resolution and inadequate target to background performance.

Advances in molecular imaging have led to the identification of several thrombus specific MR contrast agents that target either fibrin[10, 11] or activated platelets.[12] Recent clinical trial data with a fibrin-targeted gadolinium (Gd)-based probe, EP-2104R, indicated that this probe can identify thrombi in the heart chambers, carotid arteries, or aortic arch, and that the positive image contrast persists for hours.[13, 14] These clinical studies followed a series of molecular MR imaging studies of thrombosis in swine, rabbit, and pigs,[11, 15–23] but surprisingly there has been neither a study characterizing intracranial thrombus after ischemic stroke nor a literature on the efficacy of EP-2104R in rodent models of thrombosis, most likely because of the complexity of the surgical model as well as the requirement for high-field MRI. We therefore sought to evaluate the efficacy of EP-2104R for molecular imaging of intracranial thrombus at high field in a rat model of embolic stroke. For this, pre and post contrast images with EP-2104R were compared to Gd-DTPA enhanced images. Since thrombus molecular imaging may be incorporated into the stroke imaging workup, the impact of EP-2104R on diffusion weighted imaging (DWI), perfusion weighted imaging (PWI), and time of flight (TOF) angiography is also assessed.

## Methods

All experiments were performed in accordance with the NIH Guide for the Care and Use of Laboratory Animals and were approved by the Massachusetts General Hospital Subcommittee on Research Animal Care.

### Surgical Procedures

Focal embolic cerebral ischemia is produced in adult male Wistar rats (350–400 g, n=13; Charles River Laboratories, Wilmington, MA) using a previously described protocol[24]. Briefly, 24h before the ischemia surgery, animals were anesthetized by isoflurane (4–5% for induction, 1–2% for maintanance; in 30% oxygen – 70% nitrous oxide) and rectal temperature was maintained at 37.5 °C. Femoral arterial blood was collected into 20 cm-long PE50 tubing and allowed to clot first for 2h at room temperature, then for 22h at 4 °C. The next day, rats were reanesthetized, rectal temperature was maintained at 37.5 °C, and right femoral vein was cannulated for contrast agent injection. A midline incision was made in the neck and a 25 mm single thrombus that was thoroughly washed with saline and transferred to a modified PE50 catheter was injected into the right internal carotid artery at the level of the MCA. Skin incisions were closed and animal was transferred to the MR-compatible stereotaxic frame.

### Contrast Agents

EP-2104R (Epix Pharmaceuticals, Lexington MA) comprises a fibrin targeting peptide with two Gd-DOTA chelates on each of the C- and N-termini of the peptide (4 Gd in total). EP-2104R binds equally to two sites on human or rat fibrin ($K_d$ = 1.7 or 1.8 μmol/L, respectively), and has high specificity for fibrin over fibrinogen or other plasma proteins.[10] The relaxivity of EP-2104R bound to fibrin is 40.0 mmol/$L^{-1}s^{-1}$ (10.0 per Gd)10 at 4.7T.25 The commercial extracellular agent, Gd-DTPA (gadopentetate dimeglumine, Magnevist, Bayer Healthcare, Montville, NJ) was used as a control. Gd-DTPA does not bind fibrin or plasma proteins and has a relaxivity of 3.2 mmol/$L^{-1}s^{-1}$ at 4.7T in water.[26]

### MRI Protocols

All MR imaging were performed on a 4.7T small animal scanner (Bruker Biospin, Billerica, MA). Immediately after the ischemia surgery, rats were placed in the prone position in the scanner and the head was secured with a stereotaxic frame. Anesthesia was maintained with isoflurane (1–2% in 70% $N_2O$ and 30% $O_2$) and body temperature was kept at 37.5 °C by heating pad during imaging. Animals were imaged using a homemade 50×39 mm oval surface coil with the following MR sequences: 3D TOF angiography; 2D DWI; 2D T1-weighted MSME; 3D T1-weighted gradient echo (molecular MRI sequence). The field of view scanned for both 3D MRI sequences was 58×29×29 mm. The repetition time TR for the TOF sequence was 40 ms, echo time TE was 4.08 ms, flip angle was 75° and number of excitations NEX was 1 with a matrix size of 192×96×96 giving 0.30 mm/pixel resolution in a scan time of 6 min. The molecular MR sequence (TR/TE/flip=40/5.8/75°, NEX=4, matrix=300×150×150, resolution=0.193 mm/pixel and scan time=1h) was performed with inferior saturation to null inflowing arterial blood. For DWI, nine 1.5 mm axial slices were imaged with TR/TE=5000/33.4, NEX=4, FOV=22×22 mm, matrix=64×64, resolution=0.344 mm/pixel, using five b values =0.4, 574, 1147, 1720, 2335 s/$mm^2$, giving a scan time=1 min 30 s. In some instances, up to 64 averages were collected. For the T1-weighted RARE sequence, nine 1.5 mm axial slices were imaged with TR/TE=650/6.3, NEX=1, FOV=22×22 mm, matrix=128×128, resolution=0.172 mm/pixel giving a scan time=2 min 50s.

### Tissue and Blood Gd Analysis

The ipsilateral internal carotid artery and MCA containing the thrombus, contralateral internal carotid artery and MCA, as well as ipsilateral and contralateral cerebral hemispheres and blood were collected from all the animals. The tissues were homogenized in nitric acid and analyzed for Gd concentration by inductively coupled plasma-mass spectrometry (ICP-MS) using added lutetium (Lu) as an internal standard.

### Fibrin Immunostaining

After perfusion with 4% paraformaldehyde, brain was removed and processed after an overnight post-fixation at 4 °C. 5 μm-thick paraffin sections were mounted on slides and immunohistochemistry was performed using monoclonal fibrin antibody (1:25 dilution, 1h at room temperature; Accurate Chemical & Scientific Corp., Westbury, NY). Sections were counterstained with hematoxylin.

### Experimental Protocols

Imaging began approximately 20 min after delivery of the thrombus. Subsequent to collection of localizer images, a series of baseline imaging studies were performed in the following order: TOF angiography, T1-weighted MSME, 3D molecular MRI sequence, and DWI. After the baseline scans were completed, 0.4 mL of the contrast agent, either EP-2104R (10 μmol/kg, n=6) or Gd-DTPA (control; 200 μmol/kg, n=5) was injected as a bolus via the femoral vein. Post contrast agent, the same imaging sequences as baseline were repeated.

After the last scan, the animal was removed from the scanner and euthanized. The vascular and brain tissues and an aliquot of blood were collected, weighed, and processed for ICP-MS analysis.

Two additional studies were performed where the animal received both contrast agents in succession. Briefly, after surgery and baseline scanning as described above, Gd-DTPA (200 μmol/kg, iv) was given as a bolus and the post-contrast imaging sequence repeated. Then, 90 min after Gd-DTPA was administered, EP-2104R (10 μmol/kg, iv) was injected and the post-contrast scans repeated.

### Data Analysis

The images were analyzed using the program Osirix (www.osirix-viewer.com) by drawing regions of interest in the thrombus, contralateral artery and adjacent brain or muscle tissue and signal intensity (SI) was quantified for the same slice. Noise was quantified as the standard deviation (SD) of the signal measured in the air outside the animal. Apparent diffusion coefficient (ADC) maps were calculated using an in-house Matlab program by fitting the natural log of the SI as a function of b value. Contrast to noise ratios (CNR) were calculated for the difference between tissue A and tissue B using the following equation (1).

$$CNR_{(\text{tissue A/tissue B})} = [\,SI_{(\text{tissue A})} - SI_{(\text{tissue B})}\,]/SD_{(\text{air})} \quad (1)$$

Gd concentration was determined by comparing the Gd:Lu ratio to a standard curve. Concentrations are reported as nmol Gd per g tissue. Since the Gd-DTPA and EP-2104R were administered at different doses, concentrations were also expressed as percent of initial dose per gram tissue (%ID/g). Differences between two groups (pre vs. post contrast, Gd-DTPA vs. EP-2104R) were compared using repeated measures ANOVA followed by Student-Newman-Keuls post hoc test when needed. Comparison of MR signal or Gd levels between the two brain hemispheres was tested with a one-sample *t*-test with the test value (ratio between the two hemispheres) set at 1. *p*-value less than 0.05 was considered significant. Uncertainties are expressed as one standard deviation.

## Results

In all 13 animals, the acute embolic stroke model was reproduced successfully. The TOF angiograms demonstrated restricted flow to the right side of the brain in all animals, suggesting an occlusive thrombus (Figure 1A, 1B). DWI was performed pre and post injection and both showed hyperintensity in the right MCA territory suggesting an ischemic lesion in all animals imaged (Figure 1C). Likewise, the corresponding ADC maps show a lesion at the same localization (Figure 1D). In the EP-2104R injected animals the lesion size of the pre injection DWI was 5.17±1.8 % of the contralateral hemisphere and post injection DWI was 9.28±3.1 % of the contralateral hemisphere. In the Gd-DTPA injected animals the lesion size of the pre-injection DWI was 4.9±1.6 % of the contralateral hemisphere and post injection DWI was 7.12 ±3.5 % of the contralateral hemisphere. There was no difference in lesion size between EP-2104R and Gd-DTPA groups at either pre or post injection DWI scans (Repeated measures ANOVA: F=0.840, p=0.3832).

The thrombus was not directly visible on baseline scans. After injection of EP-2104R, the occlusive thrombus was clearly evident in the right internal carotid artery, near the origin of MCA, using the high-resolution molecular MRI sequence (Figure 2). In all EP-2104R injected animals, there was considerable enhancement of the thrombus compared to the pre EP-2104R image (Figure 3A; $CNR_{\text{thrombus/blood}}$ = 10.7 ± 0.8 post vs. 0.54 ± 0.71 pre; $CNR_{\text{thrombus/brain}}$

= 8.81 ± 0.58 post vs. −1.34 ± 0.41 pre; $p<0.0001$). However, the thrombus was not visible when animals were administered Gd-DTPA, and CNR values pre and post Gd-DTPA were not significantly different. The bright thrombus observed post EP-2104R exhibited a CNR that was highly significant ($p<0.0001$) compared to that measured post Gd-DTPA.

In addition to EP-2104R enhancement of the injected occlusive thrombus, additional enhancement was noted in the vessel wall proximal to the thrombus. An example of this is demonstrated in Figure 4C where a coronal maximum intensity projection shows a region of enhancement extending the length of the right carotid artery to the origin of MCA. The source images reveal the presence of an occlusive thrombus at the level of the MCA (Figure 4D–4F). Proximal to this occlusive thrombus is vessel wall enhancement (Figure 4A, 4B) that is likely fresh mural thrombus caused by endothelial damage induced during catheter delivery of the aged clot typical for this model. The vessel wall enhancement was observed in all 6 animals post EP-2104R injection but was not observed prior to EP-2104R injection or observed in the contralateral vessel. Thrombus CNR was high post EP-2104R and highly significant compared to pre EP-2104R images CNR (Figure 3B; $CNR_{thrombus:blood}$ = 22.3±3.2 post vs 3.3±0.6 pre; $CNR_{thrombus:brain}$ = 17.7±2.8 vs −1.2±0.4 pre; $p<0.005$). No significant difference in vessel wall CNR was observed following Gd-DTPA administration.

The ex vivo tissue analyses mirrored the imaging findings (Figure 3C). The Gd thrombus to blood ratio was 18.5 ± 8.7 at 90 min following EP-2104R injection, which was significantly higher than that measured after Gd-DTPA administration (2.18 ± 0.66; $p<0.05$). The concentration of Gd in the thrombus was 5.8 times higher in the EP-2104R group than the control ($p<0.05$). To determine if the blood brain barrier was compromised at this hyperacute phase of ischemia, T1-weighted imaging was performed prior to and post (15 min) contrast agent administration at the level of the lesion. No difference in signal intensity was observed between the two hemispheres of the brain following either EP-2104R or Gd-DTPA administration. Ex-vivo analysis of the left and right cortex indicated a small but significant ($p<0.025$) 2-fold increase in Gd concentration in the injured right cortex compared to the left side. The 2-fold increase was seen with both Gd-DTPA and EP-2104R. However the absolute concentration of Gd in the brain was quite low (0.47 ± 0.14 nmol/g for EP-2104R and 1.16 ± 0.42 nmol/g for Gd-DTPA) and is below the limit detectable by MRI.

Two additional animals that were imaged received Gd-DTPA and then EP-2104R 80 min later. In these animals, the thrombus was only visible post injection of EP-2104R and was not apparent on the pre-contrast images or on the images obtained up to 90 min post injection of Gd-DTPA.

In an additional animal, immunohistochemistry with monoclonal antibody revealed the presence of fibrin along the internal carotid artery wall (data not shown).

## Discussion

This study demonstrates direct, positive contrast detection of intracranial thrombi in a rat model of ischemic stroke. This model is known from ex vivo analyses to produce occlusive thrombi which result in reduced cerebral blood flow and hyperintense lesions on diffusion weighted MR images.[24] The thrombus was readily visible in all animals following EP-2104R, but was not visualized prior to contrast agent or if conventional Gd-DTPA was given. Since fibrin is present in most thrombi, fibrin-targeted molecular MRI may prove more sensitive than techniques like the hyperdense sign on CT,[2] or direct detection by MRI due to methemoglobin. As the thrombus ages, hemoglobin oxidizes to methemoglobin which has a strong T1-shortening effect. This phenomenon has been exploited in direct detection of thrombi by MRI, and used to identify complex plaque[27] and venous thromboemboli.[28] The sensitivity of the

direct thrombus detection method relies in part on the presence of methemoglobin at the time of imaging which depends on the age of the thrombus. The thrombus preparation in this model was not T1-bright indicating the absence of methemoglobin. Given the success of EP2104R in detecting thrombi outside the brain in humans and in large animal models,[13, 15–19] it is likely that the present results are translatable to clinical imaging.

EP-2104R is a Gd-based contrast agent with high affinity and selectivity for fibrin[29]. It allows visualization of fresh, as well as aged, pulmonary, coronary, cardiac, and deep vein thrombi in swine[17–19, 21–23, 30]. Phase II clinical studies in patients with venous, arterial, and cardiac thrombi showed that EP-2104R enhanced thrombi and that the signal enhancement persisted up to 24 hours after the contrast agent injection[13–14]. In spite of these extensive studies on molecular imaging of peripheral thrombus, however, there is only one published study on intracranial thrombus in which enhancement of cerebral sinus thrombus in swine was demonstrated[31]. The present study builds on this literature of direct thrombus imaging and expands the utility of EP-2104R into the detection of intracranial arterial thrombi in rats, and into thrombus imaging at high field.

The animal model used is well established in stroke research. The thrombus was aged ex vivo for 24h and imaging was performed within an hour of the thrombus being introduced into the internal carotid artery. The facile characterization of the thrombus in this study suggests that EP-2104R enhanced MRI may be a powerful tool to investigate the temporal evolution of the thrombus and characterize microemboli as the primary lesion undergoes lysis, or to investigate the effect of thrombolytic interventions.

DWI, PWI, and TOF MRA are widely used in stroke workup. In order to assess the potential impact of EP-2104R on these studies, DWI and TOF imaging was performed prior to and following EP-2104R injection. The presence of EP-2104R had no impact on the diffusion images. The MRA images were obtained about 5 min post injection and at the relatively low dose used, there was little to no venous enhancement compared to the pre EP-2104R MRA. Attempts to measure perfusion with EP-2104R were unsuccessful, presumably because of the low dose of Gd used. In two studies, rats were imaged at baseline then following Gd-DTPA (200 μmol/kg) injection and then, 80 min later, following EP-2104R injection (10 μmol/kg). The thrombus was only visible following EP-2104R administration, and the Gd-DTPA did not interfere with the EP-2104R detection of the thrombus. This finding suggests that a high dose of Gd-DTPA could be used for the perfusion study followed by EP-2104R to identify the thrombus. Alternately, the two contrast agents could be mixed together and administered at once to first acquire a perfusion map and then to identify thrombi, or simply, a higher dose of EP-2104R could be given. It is important to note in here that to compensate for the 45% lower relaxivity of EP-2104R at 4.7T compared to 1.5T,[10, 25] the dose was increased to 10 μmol/kg compared to doses of 4 and 7.5 μmol/kg used previously.[13, 17] Previous studies mainly used either a heavily T1-weighted 3D gradient echo sequence or a black blood inversion recovery sequence to detect the thrombus[30]. In this study a 3D GRE sequence with in-flow saturation was used and this approach is readily adapted to clinical imaging. The inversion recovery sequence would also likely result in high thrombus CNR.

Interestingly, EP-2104R also caused a signal enhancement along the wall of the internal carotid artery. The signal enhancement was only apparent in the vessel that was catheterized and no enhancement was observed in the contralateral artery. Vessel trauma from the catheterization procedure is known to result in fresh thrombus along the vessel wall[32] and in the present study immunohistochemistry revealed heavy staining for fibrin along the wall. The vessel itself remained patent and such mural thrombi would not be visible on angiograms. This finding further highlights the potential of molecular MRI to provide additional layers of biochemical information to the anatomical image. It also reveals the potential acute vessel damage

associated with catheterization; given the widespread use of this animal model, further characterization of endothelial impact may be warranted.

Fibrin is detected in every thrombus retrieved from acute stroke patients [33], although its amount in each thrombus varies, not only by the age of the thrombus but also by its nature. Fibrin is the predominant component of acute and organized thrombi 34 but with aging the thrombus undergoes degradation 35. The critical question is how much aging? Radioimmunoimaging with a fibrin-specific monoclonal antibody showed that the concentration in fresh and up to 5 day-old thrombi were comparable 36. Molecular MR imaging of fibrin provides more detailed information on this; signal enhancement occurs in fresh thrombus and declines as the age of thrombus past 4 weeks [37]. Previous work showed EP-2104R enhanced MRI could detect chronic human thrombectomy samples (4 weeks to 1.5 yrs old) that were implanted in the atria[19] or lungs30 of swine, as well as freshly prepared thrombi. Based on this body of prior work, it is highly likely that EP-2104R will cause similar degree of signal enhancement on fresh and aged thrombi in the brain. Indeed, our auxiliary finding of carotid vessel wall enhancement supports this assumption. However, it is important to demonstrate the time window of efficacy of EP-2104R in fresh and aged intracranial thrombi in future studies.

There are some limitations to the present study, notably the small sample size and the arbitrary time window for imaging. Animals were imaged immediately after thrombus injection, and the effective time window of imaging after thromboembolic stroke was not determined. The model utilized an occlusive, aged thrombus and also resulted in fresh thrombus along the arterial wall, however like most animal models this does not completely mimic the clinical setting. Further studies are warranted to determine the efficacy of EP-2104R in identifying intracranial thrombi in a clinical setting and to establish its sensitivity and specificity. Further imaging studies should also include a perfusion component which may be enabled by an additional dose of Gd-DTPA or a higher dose of EP-2104R.

In the management of stroke, identification of the culprit thrombotic lesion, any downstream micro-emboli, and the source of the embolus are all critical. The properties of EP-2104R such as its ability to bind to fibrin in thrombi for long periods of time, the high CNR obtained for clot to blood pool, its relatively low dose, and its lack of interference with DWI, PWI and angiography sequences, make it a potentially valuable tool in the stroke imaging workup. In previous studies including recent work in humans EP-2104R was shown to enhance cardiac, aortic, and carotid thrombi and that the enhancement persists for hours. One potential application of this probe would be a single injection followed by a multistation imaging study to characterize the primary lesion, search for intracranial microemboli, and then search for the source of the thrombus in the carotid artery, thoracic aorta, and cardiac chambers.

## Conclusion

Fibrin-specific molecular MRI allows visualization of occlusive and mural thrombi with high positive image contrast.

## Acknowledgments

This study was supported by the National Institute of Biomedical Imaging and Bioengineering (EB009062). I.A. was supported by a T32 Ruth L. Kirschstein National Research Service Award (5T32CA009502). A.G.S. was supported by PHS NS38477. Partial support was also provided by National Center for Research Resources (P41-RR14075) and the MIND Institute.

We thank Dr. Christian Farrar for his assistance with MRI.

## References


1. Donnan GA, Fisher M, Macleod M, Davis SM. Stroke. Lancet 2008;371:1612–1623. [PubMed: 18468545]
2. Leys D, Pruvo JP, Godefroy O, Rondepierre P, Leclerc X. Prevalence and significance of hyperdense middle cerebral artery in acute stroke. Stroke 1992;23:317–324. [PubMed: 1542889]
3. Tomsick TA, Brott TG, Olinger CP, Barsan W, Spilker J, Eberle R, Adams H. Hyperdense middle cerebral artery: Incidence and quantitative significance. Neuroradiology 1989;31:312–315. [PubMed: 2797422]
4. Goldmakher GV, Camargo EC, Furie KL, Singhal AB, Roccatagliata L, Halpern EF, Chou MJ, Biagini T, Smith WS, Harris GJ, Dillon WP, Gonzalez RG, Koroshetz WJ, Lev MH. Hyperdense basilar artery sign on unenhanced ct predicts thrombus and outcome in acute posterior circulation stroke. Stroke 2009;40:134–139. [PubMed: 19038918]
5. Krings T, Noelchen D, Mull M, Willmes K, Meister IG, Reinacher P, Toepper R, Thron AK. The hyperdense posterior cerebral artery sign: A computed tomography marker of acute ischemia in the posterior cerebral artery territory. Stroke 2006;37:399–403. [PubMed: 16397187]
6. Leary MC, Kidwell CS, Villablanca JP, Starkman S, Jahan R, Duckwiler GR, Gobin YP, Sykes S, Gough KJ, Ferguson K, Llanes JN, Masamed R, Tremwel M, Ovbiagele B, Vespa PM, Vinuela F, Saver JL. Validation of computed tomographic middle cerebral artery "Dot"Sign: An angiographic correlation study. Stroke 2003;34:2636–2640. [PubMed: 14593125]
7. Manelfe C, Larrue V, von Kummer R, Bozzao L, Ringleb P, Bastianello S, Iweins F, Lesaffre E. Association of hyperdense middle cerebral artery sign with clinical outcome in patients treated with tissue plasminogen activator. Stroke 1999;30:769–772. [PubMed: 10187877]
8. Mattle HP, Arnold M, Georgiadis D, Baumann C, Nedeltchev K, Benninger D, Remonda L, von Budingen C, Diana A, Pangalu A, Schroth G, Baumgartner RW. Comparison of intraarterial and intravenous thrombolysis for ischemic stroke with hyperdense middle cerebral artery sign. Stroke 2008;39:379–383. [PubMed: 18096842]
9. Qureshi AI, Ezzeddine MA, Nasar A, Suri MF, Kirmani JF, Janjua N, Divani AA. Is iv tissue plasminogen activator beneficial in patients with hyperdense artery sign? Neurology 2006;66:1171–1174. [PubMed: 16636232]
10. Overoye-Chan K, Koerner S, Looby RJ, Kolodziej AF, Zech SG, Deng Q, Chasse JM, McMurry TJ, Caravan P. Ep-2104r: A fibrin-specific gadolinium-based mri contrast agent for detection of thrombus. J Am Chem Soc 2008;130:6025–6039. [PubMed: 18393503]
11. Flacke S, Fischer S, Scott MJ, Fuhrhop RJ, Allen JS, McLean M, Winter P, Sicard GA, Gaffney PJ, Wickline SA, Lanza GM. Novel mri contrast agent for molecular imaging of fibrin implications for detecting vulnerable plaques. Circulation 2001;104:1280–1285. [PubMed: 11551880]
12. von zur Muhlen C, von Elverfeldt D, Moeller JA, Choudhury RP, Paul D, Hagemeyer CE, Olschewski M, Becker A, Neudorfer I, Bassler N, Schwarz M, Bode C, Peter K. Magnetic resonance imaging contrast agent targeted toward activated platelets allows in vivo detection of thrombosis and monitoring of thrombolysis. Circulation 2008;118:258–267. [PubMed: 18574047]
13. Spuentrup E, Botnar RM, Wiethoff AJ, Ibrahim T, Kelle S, Katoh M, Oezgun M, Nagel E, Vymazal J, Graham PB, Gunther RW, Maintz D. Mr imaging of thrombi using ep-2104r, a fibrin-specific contrast agent: Initial results in patients. Eur Radiol 2008;18:1995–2005. [PubMed: 18425519]
14. Vymazal J, Spuentrup E, Cardenas-Molina G, Wiethoff AJ, Hartmann MG, Caravan P, Parsons EC Jr. Thrombus imaging with fibrin-specific gadolinium-based mr contrast agent ep-2104r: Results of a phase ii clinical study of feasibility. Invest Radiol 2009;44:697–704. [PubMed: 19809344]
15. Stracke CP, Katoh M, Wiethoff AJ, Parsons EC, Spangenberg P, Spuntrup E. Molecular mri of cerebral venous sinus thrombosis using a new fibrin-specific mr contrast agent. Stroke 2007;38:1476–1481. [PubMed: 17379818]
16. Spuentrup E, Katoh M, Buecker A, Fausten B, Wiethoff AJ, Wildberger JE, Haage P, Edward CP, Botnar RM, Graham PB, Vettelsehoss M, Gunther RW. Molecular mr imaging of human thrombi in a swine model of pulmonary embolism using a fibrin-specific contrast agent. Invest Radiol 2007;42:586–595. [PubMed: 17620942]

17. Spuentrup E, Katoh M, Wiethoff AJ, Parsons EC Jr, Botnar RM, Mahnken AH, Gunther RW, Buecker A. Molecular magnetic resonance imaging of pulmonary emboli with a fibrin-specific contrast agent. Am J Respir Crit Care Med 2005;172:494–500. [PubMed: 15937292]

18. Spuentrup E, Buecker A, Katoh M, Wiethoff AJ, Parsons EC Jr, Botnar RM, Weisskoff RM, Graham PB, Manning WJ, Gunther RW. Molecular magnetic resonance imaging of coronary thrombosis and pulmonary emboli with a novel fibrin-targeted contrast agent. Circulation 2005;111:1377–1382. [PubMed: 15738354]

19. Spuentrup E, Fausten B, Kinzel S, Wiethoff AJ, Botnar RM, Graham PB, Haller S, Katoh M, Parsons EC Jr, Manning WJ, Busch T, Gunther RW, Buecker A. Molecular magnetic resonance imaging of atrial clots in a swine model. Circulation 2005;112:396–399. [PubMed: 16009790]

20. Sirol M, Fuster V, Badimon JJ, Fallon JT, Moreno PR, Toussaint JF, Fayad ZA. Chronic thrombus detection with in vivo magnetic resonance imaging and a fibrin-targeted contrast agent. Circulation 2005;112:1594–1600. [PubMed: 16145001]

21. Botnar RM, Buecker A, Wiethoff AJ, Parsons EC Jr, Katoh M, Katsimaglis G, Weisskoff RM, Lauffer RB, Graham PB, Gunther RW, Manning WJ, Spuentrup E. In vivo magnetic resonance imaging of coronary thrombosis using a fibrin-binding molecular magnetic resonance contrast agent. Circulation 2004;110:1463–1466. [PubMed: 15238457]

22. Spuentrup E, Katoh M, Wiethoff AJ, Buecker A, Botnar RM, Parsons EC, Guenther RW. Molecular coronary mr imaging of human thrombi using ep-2104r, a fibrin-targeted contrast agent: Experimental study in a swine model. Rofo 2007;179:1166–1173. [PubMed: 17948194]

23. Katoh M, Haage P, Wiethoff AJ, Gunther RW, Bucker A, Tacke J, Spuentrup E. Molecular magnetic resonance imaging of deep vein thrombosis using a fibrin-targeted contrast agent: A feasibility study. Invest Radiol. 2009

24. Zhang RL, Chopp M, Zhang ZG, Jiang Q, Ewing JR. A rat model of focal embolic cerebral ischemia. Brain Res 1997;766:83–92. [PubMed: 9359590]

25. Caravan P, Farrar CT, Frullano L, Uppal R. Influence of molecular parameters and increasing magnetic field strength on relaxivity of gadolinium- and manganese-based t1 contrast agents. Contrast Media Mol Imaging. 2009

26. Rohrer M, Bauer H, Mintorovitch J, Requardt M, Weinmann HJ. Comparison of magnetic properties of mri contrast media solutions at different magnetic field strengths. Invest Radiol 2005;40:715–724. [PubMed: 16230904]

27. Moody AR, Murphy RE, Morgan PS, Martel AL, Delay GS, Allder S, MacSweeney ST, Tennant WG, Gladman J, Lowe J, Lowe J, Hunt BJ. Characterization of complicated carotid plaque with magnetic resonance direct thrombus imaging in patients with cerebral ischemia. Circulation 2003;107:3047–3052. [PubMed: 12796133]

28. Kelly J, Rudd A, Lewis RR, Coshall C, Moody A, Hunt BJ. Venous thromboembolism after acute ischemic stroke: A prospective study using magnetic resonance direct thrombus imaging. Stroke 2004;35:2320–2325. [PubMed: 15322298]

29. Overoye-Chan K, Koerner S, Looby RJ, Kolodziej AF, Zech SG, Deng Q, Chasse JM, McMurry TJ, Caravan P. Ep-2104r: A fibrin-specific gadolinium-based mri contrast agent for detection of thrombus. J Am Chem Soc 2008;130:6025–6039. [PubMed: 18393503]

30. Spuentrup E, Katoh M, Buecker A, Fausten B, Wiethoff AJ, Wildberger JE, Haage P, Parsons EC Jr, Botnar RM, Graham PB, Vettelschoss M, Gunther RW. Molecular mr imaging of human thrombi in a swine model of pulmonary embolism using a fibrin-specific contrast agent. Invest Radiol 2007;42:586–595. [PubMed: 17620942]

31. Stracke CP, Katoh M, Wiethoff AJ, Parsons EC, Spangenberg P, Spuntrup E. Molecular mri of cerebral venous sinus thrombosis using a new fibrin-specific mr contrast agent. Stroke 2007;38:1476–1481. [PubMed: 17379818]

32. Hatton MW, Ross B, Timleck M, Southward SM, Richardson M. Turnover and fate of fibrinogen and platelets at the rabbit aorta wall immediately after a balloon de-endothelializing injury in vivo. Thromb Haemost 2006;96:60–67. [PubMed: 16807652]

33. Marder VJ, Chute DJ, Starkman S, Abolian AM, Kidwell C, Liebeskind D, Ovbiagele B, Vinuela F, Duckwiler G, Jahan R, Vespa PM, Selco S, Rajajee V, Kim D, Sanossian N, Saver JL. Analysis of

thrombi retrieved from cerebral arteries of patients with acute ischemic stroke. Stroke 2006;37:2086–2093. [PubMed: 16794209]

34. Bini A, Fenoglio J Jr, Sobel J, Owen J, Fejgl M, Kaplan KL. Immunochemical characterization of fibrinogen, fibrin i, and fibrin ii in human thrombi and atherosclerotic lesions. Blood 1987;69:1038–1045. [PubMed: 2950941]
35. Francis CW, Markham RE Jr, Marder VJ. Demonstration of in situ fibrin degradation in pathologic thrombi. Blood 1984;63:1216–1224. [PubMed: 6231967]
36. Rosebrough SF, Grossman ZD, McAfee JG, Kudryk BJ, Subramanian G, Ritter-Hrncirik CA, Witanowski LS, Tillapaugh-Fay G, Urrutia E. Aged venous thrombi: Radioimmunoimaging with fibrin-specific monoclonal antibody. Radiology 1987;162:575–577. [PubMed: 3797675]
37. Sirol M, Fuster V, Badimon JJ, Fallon JT, Moreno PR, Toussaint JF, Fayad ZA. Chronic thrombus detection with in vivo magnetic resonance imaging and a fibrin-targeted contrast agent. Circulation 2005;112:1594–1600. [PubMed: 16145001]

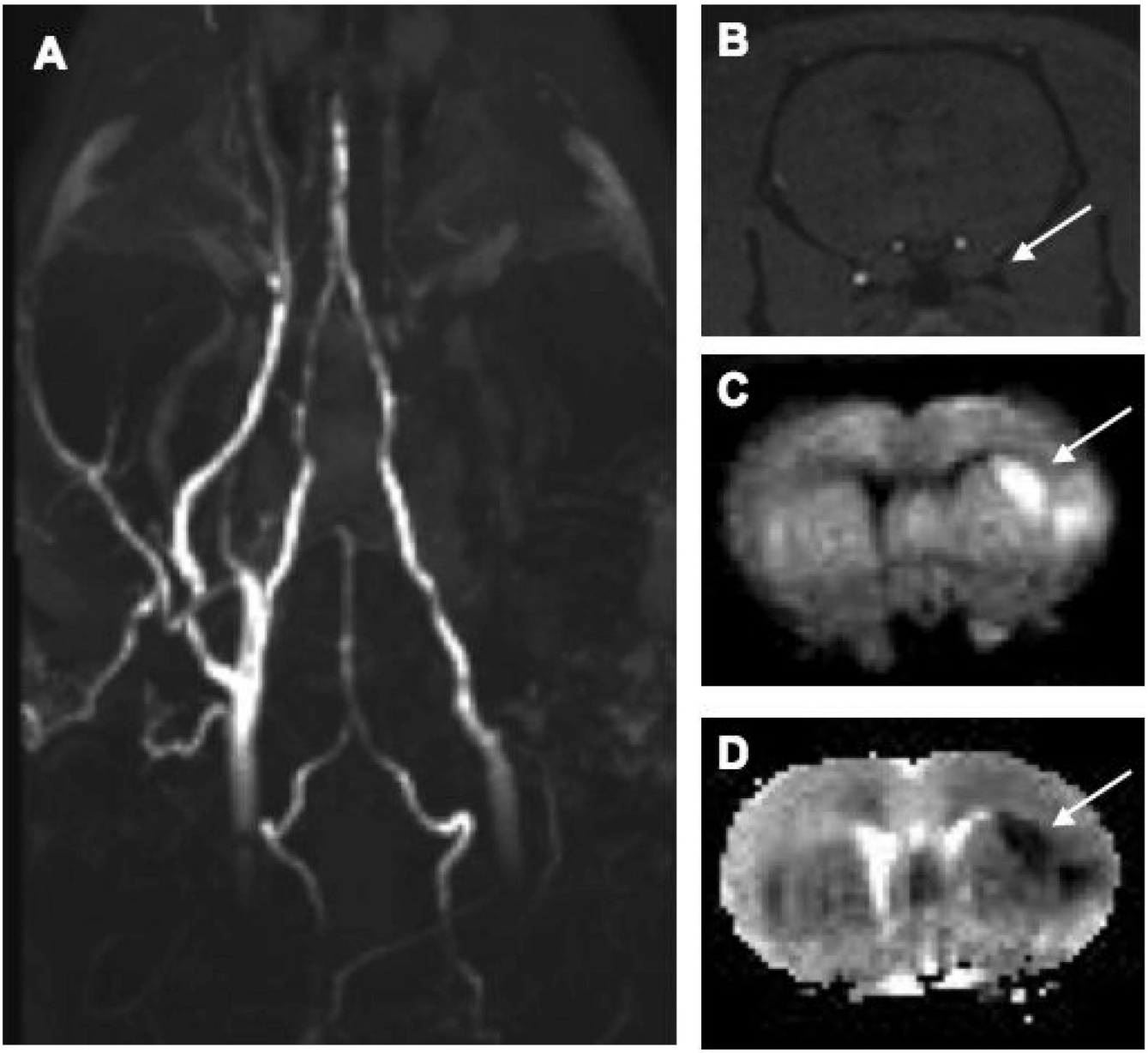


**Figure 1.**

(A) Coronal maximum intensity projection of time-of-flight angiogram shows right side flow deficit. (B) Axial slice from the 3D time of flight angiogram shows no flow in the right internal cmiddle cerebral artery (arrow). (C) Diffusion weighted image at same level shows a hyperintense lesion in the MCA territory that is also obvious on the corresponding ADC map (D) with a calculated ADC of $0.324 \pm 0.043 \times 10^{-3}$ $mm^2/s$.

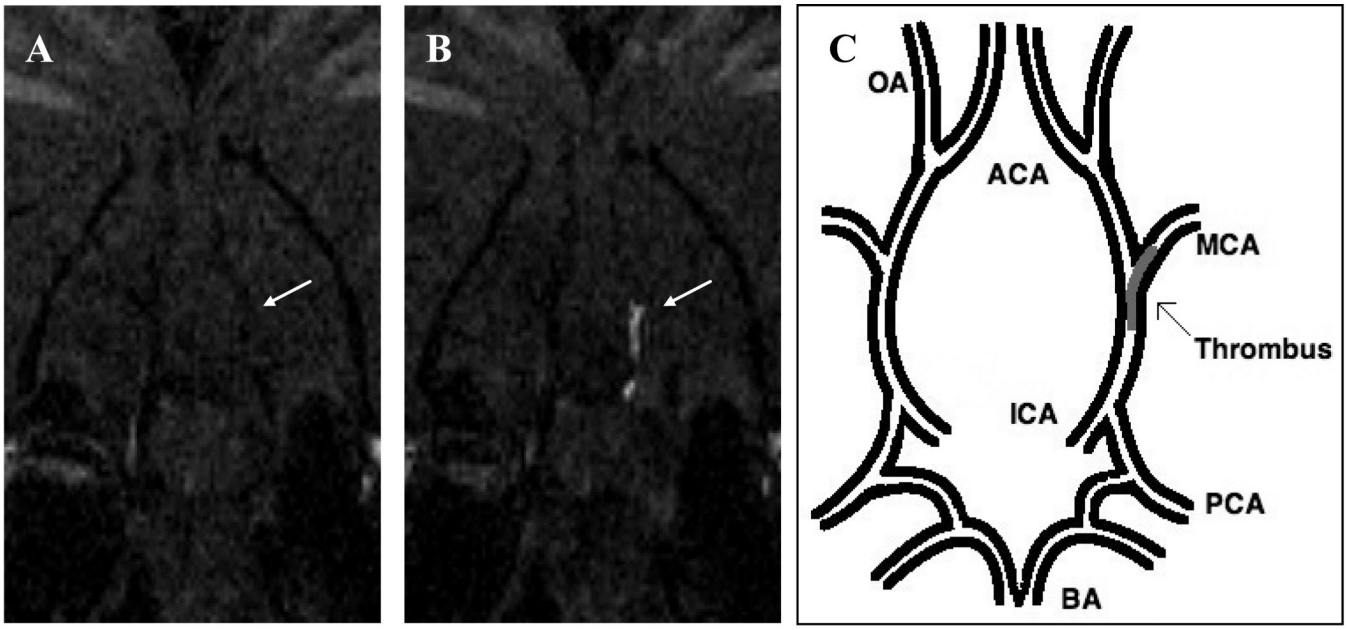


**Figure 2.**

Coronal slice from 3D T1-weighted images at level of the middle cerebral artery origin: the EP-2104R enhanced image (B) clearly identifies the thrombus (arrow) that was not visible on the image acquired prior to EP-2104R injection (A). (C) Pictorial representation of the location of the thrombus within the cerebral arterial tree. BA indicates basilar artery; PCA, posterior cerebral artery; ICA, internal carotid artery; MCA, middle cerebral artery; OA, olfactory artery; ACA, anterior cerebral artery.

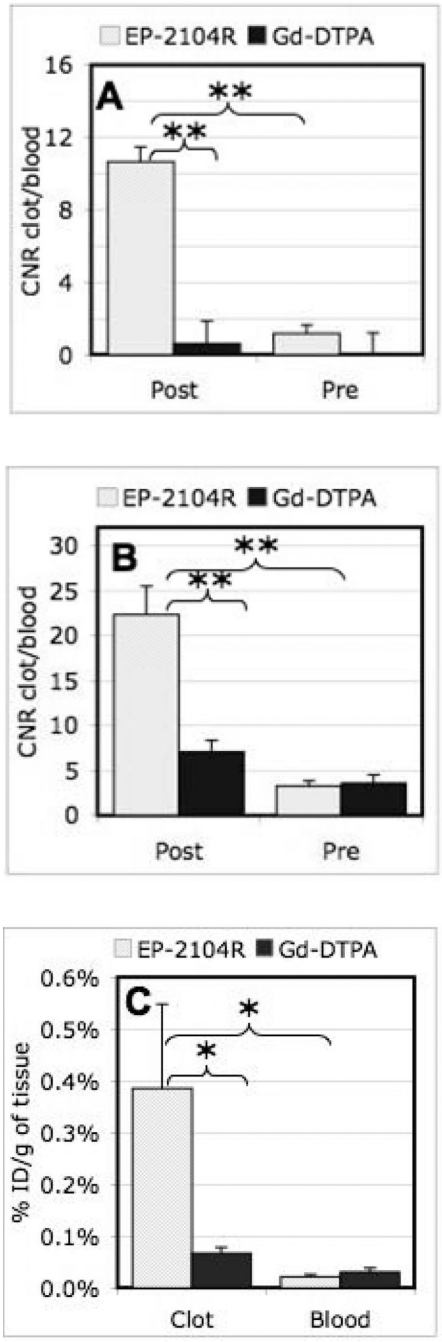


**Figure 3.**

(A) Clot to blood CNR for the aged thrombus comparing pre-injection to post injection for EP-2104R quantifies the considerable thrombus enhancement, while no increase in CNR is seen after Gd-DTPA injection. (B) Clot to blood CNR for the fresh mural thrombus caused by endothelial damage induced during catheter delivery of the aged clot. The CNR values are significantly higher post injection of EP-2104R as compared to pre-injection and Gd-DTPA injection. (C) Ex vivo Gd analysis of thrombus and blood for both EP-2104R and Gd-DTPA administration. The Gd concentration in the clot is ~18 times higher than in the blood for EP-2104R; however, the values for clot and blood are similar in the case of Gd-DTPA injection.

Repeated measures ANOVA with post hoc Student-Newman-Keuls test: * $p < 0.05$; ** $p < 0.005$.

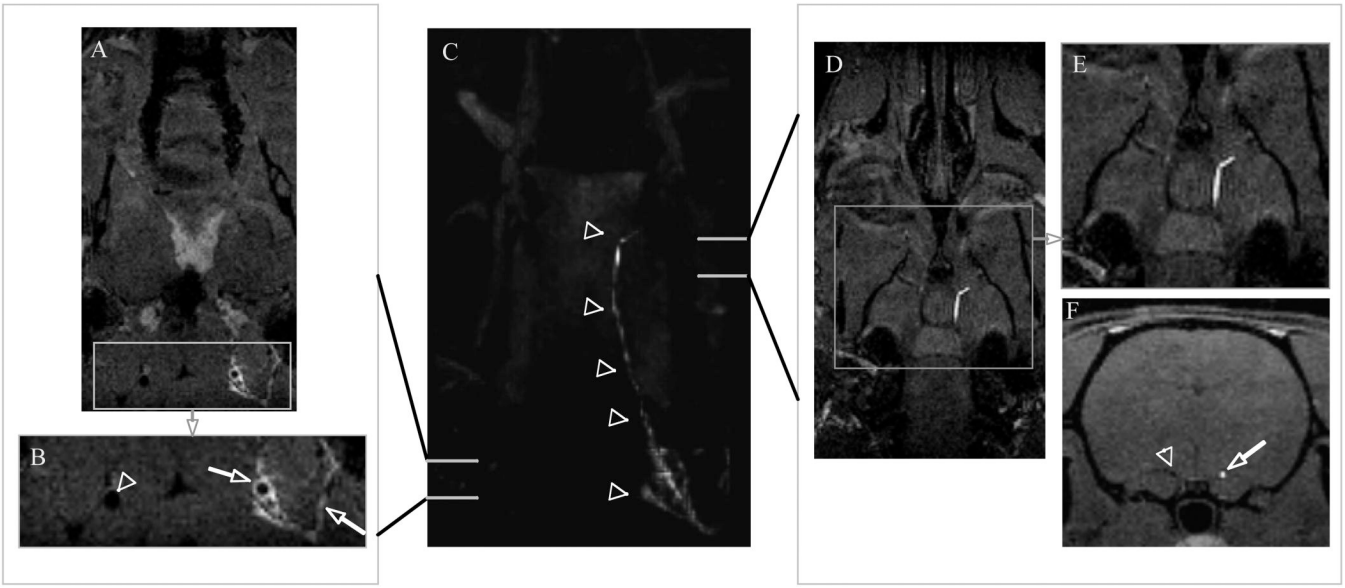


**Figure 4.**

Center panel (C) coronal maximum intensity projection showing a region of enhancement extending the length of the right carotid artery to middle cerebral bifurcation depicted by arrowheads. Left panel: (A) Source image and (B) enlargement of boxed area in (A) anterior to the carotid bifurcation showing vessel wall enhancement, likely mural thrombus (arrow), in the right internal carotid artery and enhanced clotted side branches (arrow) while contralateral carotid (arrowhead) shows no vessel wall enhancement. Right panel: (D) source image and (E) enlargement of boxed area in (D) at level of MCA origin revealing the presence of an occlusive thrombus; (F) axial reformat demonstrating occlusive thrombus (arrow) and patent contralateral artery (arrowhead).